

Mechanisms in Environmentally-Assisted One-photon Phase Control

Leonardo A. Pachón^{1,2} and Paul Brumer¹

¹*Chemical Physics Theory Group, Department of Chemistry and Center for Quantum Information and Quantum Control, University of Toronto, Toronto, Canada M5S 3H6*

²*Grupo de Física Atómica y Molecular, Instituto de Física, Facultad de Ciencias Exactas y Naturales, Universidad de Antioquia UdeA; Calle 70 No. 52-21, Medellín, Colombia*

(Dated: 27 September 2018)

The ability of an environment to assist in one-photon phase control relies upon entanglement between the system and bath and on the breaking of the time reversal symmetry. Here, one photon phase control is examined analytically and numerically in a model system, allowing an analysis of the relative strength of these contributions. Further, the significant role of non-Markovian dynamics and of moderate system-bath coupling in enhancing one-photon phase control is demonstrated, and an explicit role for quantum mechanics is noted in the existence of initial non-zero stationary coherences. Finally, desirable conditions are shown to be required to observe such environmentally assisted control, since the system will naturally equilibrate with its environment at longer times, ultimately resulting in the loss of phase control.

I. INTRODUCTION

The coherent control of molecular processes has been highly successful, both computationally and experimentally, when applied to isolated molecular systems¹. Indeed, a wide variety of scenarios has been proposed ranging from the control of products in the continuum, such as photodissociation, to bound state control of radiationless transitions²⁻⁴. By contrast, control of a system in the presence of an environment, where decoherence effects often destroy coherences^{5,6}, is only in its early stages of development. To this end, one photon phase control, the subject of this paper, is of particular interest insofar as the environment *assists*, rather than impedes, control of the system dynamics.

One photon phase control has been the subject of considerable recent discussion and attention⁷⁻¹⁷. In this one photon phase control (OPPC) scenario, control is achieved by varying the spectral phase of a weak pulse while keeping its power spectrum fixed. Particular interest in this scenario arises from a seminal proof in which it was shown that OPPC was not possible for isolated molecular systems in which control was over products in the continuum¹⁸. However, subsequent experiments on control of retinal isomerization in bacteriorhodopsin in the weak regime⁷ as well as in the strong field regime¹⁰ motivated controversy^{8-10,14} and the need for clarification of conditions under which such control was possible.

This clarification, provided in Refs. 12 and 17, showed that control was *possible* for both isolated systems and open quantum systems under well defined conditions. In particular, for an observable \hat{O} of a physicochemical system defined by the Hamiltonian \hat{H}_S , it was shown that: (i) if the system is isolated and initially devoid of coherence then one-photon phase control is possible only if $[\hat{H}_S, \hat{O}] \neq 0$, but (ii) if the system is coupled to an environment, as in any realistic case, then control is possible not only if $[\hat{H}_S, \hat{O}] \neq 0$, but even if $[\hat{H}_S, \hat{O}] = 0$, in which case it is *environmentally assisted*^{12,16,17}. As it was noted in Refs. 12 and 17, the case of $[\hat{H}_S, \hat{O}] \neq 0$ includes, e.g., isomerization since the probability of observing an isomer is an observable that does not commute with \hat{H}_S .

The aim of Ref. 12 was to establish these general commutation-based rules, whereas Ref. 17 identified the physical processes responsible for OPPC. In particular, based on a general master equation approach, we qualitatively identified two main mechanisms for OPPC in open systems: the breaking of time-reversal symmetry and the entanglement between the system and the bath. These two mechanisms differ in character; the time-reversal symmetry

does not rely upon quantum mechanics, whereas the initial correlations between the system and the bath are quantum in nature¹⁹. These mechanisms also work on different time scales, the initial correlations contribute in the short time regime while the time-reversal symmetry dominates in the long time regime. As such, it is the latter that determines the amount of control that can be achieved within this control scheme.

In this paper, we quantitatively analyze the magnitude of each of these contributions and demonstrate the significant role of the non-Markovian dynamics and of moderate system-bath coupling in enhancing the extent of one-photon phase control. Note that the system-bath interaction plays a dual role in the OPPC scenario. First, it assists insofar as allowing phase control for systems where such control would not occur if the system were isolated. However, since the system-bath coupling persists long after the laser pulse, it induces relaxation to equilibrium at long times, resulting in long-time loss of phase control. Hence, as we show below, maintaining phase control over an extended period of time requires careful balancing of the system-bath interactions.

II. INITIAL CONSIDERATIONS

Consider a quantum system S described by the Hamiltonian \hat{H}_S with $\hat{H}_S|n\rangle = E_n|n\rangle$. We consider below two cases, where the system is isolated and irradiated with a laser, and the second where the system is irradiated in the presence of an environment (or “bath”). In the latter case, the full Hamiltonian is given by $\hat{H} = \hat{H}_S + \hat{V}_L + \hat{H}_B + \hat{H}_{SB}$, where \hat{V}_L denotes the term laser, \hat{H}_B is the Hamiltonian of the environment and \hat{H}_{SB} is the system-bath coupling.

A. Initial Considerations on System Dynamics

Under the influence of time-dependent fields and in the presence of an environment, the time evolution of the system density-operator $\hat{\rho}_S$ is given by²⁰

$$\begin{aligned} \langle n|\hat{\rho}_S(t)|m\rangle &= \sum_{\nu} J_{nm;\nu\nu}(t)\langle\nu|\hat{\rho}_S(0)|\nu\rangle \\ &+ \sum_{\nu\neq\mu} J_{nm;\nu\mu}(t)\langle\nu|\hat{\rho}_S(0)|\mu\rangle, \end{aligned} \tag{1}$$

where $J_{nm;\nu\mu}(t)$ denotes the propagation function in the system energy basis representation²⁰. As such, the system dynamics is contained in the propagation function elements $J_{nm;\nu\mu}(t)$ that can be derived, as in Ref. 20, from a path integral representation of the propagation function. The first two indices nm denote the density matrix element in which we are interested and the last two indices $\nu\mu$ refer to the elements of the initial density matrix that contribute, as shown in Eq. (1), to the dynamics of the nm -th element. The general picture implied by Eq. (1) is that the time evolution of the diagonal elements $n = m$ (populations) as well as the off-diagonal elements (coherences) of the density matrix depends linearly on the initial diagonal and off-diagonal elements.

To explore the physical meaning and role of the $J_{nm;\nu\mu}(t)$ consider first the case of unitary time-evolution in absence of time dependent external forces. Examining this case allows a reinterpretation of some of the known features of unitary dynamics in terms of this formalism. In the case of unitary time-evolution, the elements of the propagating function in Eq. (1) reduce to the familiar expression

$$J_{nm;\nu\mu}(t) = e^{-i(E_m - E_n)t/\hbar} \delta_{n\nu} \delta_{m\mu}. \quad (2)$$

The Kronecker deltas prevent (a) the transfer of initial population from $\langle \nu | \hat{\rho}_S(0) | \nu \rangle$ to $\langle n | \hat{\rho}_S(t) | n \rangle$ mediated by $J_{nm;\nu\nu}(t)$, as well as (b) the generation of coherences, $n \neq m$, from initial populations $\langle \nu | \hat{\rho}_S(0) | \nu \rangle$. In addition, the possibility of controlling the populations at time t , i.e., the $\langle n | \hat{\rho}_S(t) | n \rangle$, by varying the initial coherences $\langle \nu | \hat{\rho}_S(0) | \mu \rangle$, $\nu \neq \mu$, a possible control objective, is also prevented during the unitary time evolution governed by Eq. (2).

In the presence of time dependent external fields or of an external environment, the propagating function elements $J_{nm;\nu\mu}(t)$ differ from those in Eq. (2), as discussed below. Although the particular form of the $J_{nm;\nu\mu}(t)$ depends upon the environment and on the external field, generally the Kronecker delta restrictions will disappear, allowing for the transfer of population, the generation of coherences and the contribution of the initial coherences to the time evolution of the populations. Specifically, in the presence of dissipation, the delta functions in Eq. (2) broaden, allowing for the additional processes discussed below. In Ref. 20 we provide a deeper description of these extra processes in the context of incoherent excitation of open quantum systems²⁰⁻²⁴. These effects are quantitatively considered, for OPPC, below.

B. Initial Considerations on Control

Consider now controlling the expectation value of a system observable \hat{O} . In general, the time evolution of the expectation value \hat{O} can be expressed as $\langle \hat{O}(t) \rangle = \sum_{n,m} \langle n | \hat{O} | m \rangle \langle m | \hat{\rho}_S(t) | n \rangle$. We are particularly interested in observables where $[\hat{O}, \hat{H}_S] = 0$, i.e. those that are not phase controllable^{12,17} in isolated systems. In this case, $\langle \hat{O}(t) \rangle = \sum_n \langle n | \hat{O} | n \rangle \langle n | \rho_S(t) | n \rangle$. Using Eq. (1), we obtain

$$\begin{aligned} \langle \hat{O}(t) \rangle &= \sum_{n,\nu} \langle n | \hat{O} | n \rangle J_{nn;\nu\nu}(t) \langle \nu | \hat{\rho}_S(0) | \nu \rangle \\ &+ \sum_{n,\nu \neq \mu} \langle n | \hat{O} | n \rangle J_{nn;\nu\mu}(t) \langle \nu | \hat{\rho}_S(0) | \mu \rangle. \end{aligned} \quad (3)$$

First consider one-photon phase control from states initially devoid of coherence, i.e., $\langle \nu | \hat{\rho}_S(0) | \mu \rangle = 0$ for $\nu \neq \mu$. Under these circumstances, and with the assumption of irradiation with *weak* laser fields, one-photon phase control is not possible if the molecule is isolated, i.e., if the dynamics is unitary^{12,17}. By contrast, for the case of non-unitary dynamics (the open system case), environmentally assisted control is possible^{12,17}.

Below, we examine the origin and nature of this effect. Although Eq. (3) is general, we anticipate two physical mechanisms that could be responsible for one-photon phase control in the open-system case. The first arises from the fact that, in the presence of the environment, the stationary states of the system are no longer diagonal in the system's Hamiltonian eigenbasis $\{|n\rangle\}$. Specifically, interaction with the environment produces off-diagonal elements in the initial system density operator $\hat{\rho}_S(0)$ which, by virtue of Eq. (3), will contribute to the evolution of the expectation value of \hat{O} . The second relates to time-reversal-symmetry breaking. For unitary evolution, one can decompose $J_{nn;\nu\nu}(t)$ into two terms, one related to the process $|\nu\rangle \rightarrow |n\rangle$ and another term related to the dual process, $\langle n| \leftarrow \langle \nu|$. These two processes “interfere destructively” in $J_{nn;\nu\nu}(t)$. However, in the particular case of an open system this symmetry is broken, allowing for the encoding of phase information in $J_{nn;\nu\nu}(t)$, as noted below.

A detailed analysis of phase control in an isolated and model system follows below.

III. UNITARY EVOLUTION AND ONE-PHOTON PHASE-CONTROL

To examine one-photon phase control we consider an analytically soluble model for both the unitary and non-unitary cases. In particular, consider the vibrations of a diatomic molecule of frequency $\omega_0 = \sqrt{k/m}$, where m is the reduced mass and k the coupling constant between the atoms. Although an apparently simple model, it will be seen to provide great insight into the physics of phase control. It also provides a model for a wide variety of physical systems such as nano-mechanical resonators, trapped ions, membranes, optical mirrors, etc.²⁵.

For the unitary case, the Hamiltonian is given by

$$\hat{H} = \hat{H}_S + \hat{V}_L = \frac{\hat{p}^2}{2m} + \frac{m\omega_0^2}{2}\hat{q}^2 + \hat{q}E(t), \quad (4)$$

where $E(t)$ denotes the electric field of the laser pulse. This Hamiltonian describes then a linearly-forced harmonic oscillator. The Fourier transform of the electric field is $\tilde{E}(\omega) = \sqrt{|S(\omega)|} \exp[-i\varphi(\omega)]$, where $S(\omega)$ is the field amplitude and $\varphi(\omega)$ is the spectral phase. ‘‘Phase control’’ refers to the effects on the molecular dynamics of manipulating the spectral phase $\varphi(\omega)$, while keeping $S(\omega)$ fixed.

A. System Unitary Time Evolution

In the position representation, the time evolution of the system-density-matrix element $\rho_S(\mathbf{q}', 0) = \langle q'_+ | \hat{\rho}_S(0) | q'_- \rangle$ can be derived from

$$\rho_S(\mathbf{q}'', t) = \int dq' J(\mathbf{q}'', t; \mathbf{q}', 0) \rho_S(\mathbf{q}', 0), \quad (5)$$

where $J(\mathbf{q}'', t; \mathbf{q}', 0)$ is the propagating function, which for the case of unitary time-evolution is $J(\mathbf{q}'', t; \mathbf{q}', 0) = U(q''_+, q'_+, t) U^*(q''_-, q'_-, t)$, with $U(q''_+, q'_+, t) = \langle q''_+ | \hat{U}(t) | q'_+ \rangle$ and $\hat{U}(t) = \hat{\mathcal{T}} \exp[-i \int_{t_0}^t ds \hat{H}(s)/\hbar]$, $\hat{\mathcal{T}}$ being the time-ordering operator^{26–28}. For the unitary case, with time evolution operator $\hat{U}(t)$, one can obtain the propagating function elements $J_{nm;\nu\mu}(t)$ in Eq. (1) by projecting onto the system energy basis²⁰. For the particular case in Eq. (4), the unitary time evolution can be obtained analytically (c.f. Chap. 3 in Ref. 26 or Chap. 2 in Ref. 27), giving analytic propagating function elements.

For the purpose of discussion, consider the case where the system is prepared in a coherent superposition of the ground and first excited states, i.e., $\hat{\rho}_s(0) = (|0\rangle\langle 0| + |0\rangle\langle 1| + |1\rangle\langle 0| + |1\rangle\langle 1|) / 2$. From Eq. (3), we have

$$\langle \hat{O}(t) \rangle = \frac{1}{2} \sum_{\substack{n \\ \nu, \mu=0,1}} \langle n | \hat{O} | n \rangle J_{nn;\nu\mu}(t), \quad (6)$$

where

$$J_{nn;00}(t) = \frac{1}{n! \mathcal{E}_0^{2n}} |\mathcal{E}(t)|^{2n} \exp \left\{ -\frac{|\mathcal{E}(t)|^2}{\mathcal{E}_0^2} \right\}, \quad (7)$$

$$J_{nn;01}(t) = \frac{1}{n! \mathcal{E}_0^{2n+1}} |\mathcal{E}(t)|^{2n-2} \exp \left\{ -\frac{|\mathcal{E}(t)|^2}{\mathcal{E}_0^2} \right\} \\ \times \mathcal{E}(t) \{ -2n\mathcal{E}_0^2 + |\mathcal{E}(t)|^2 \}, \quad (8)$$

$$J_{nn;11}(t) = \frac{1}{n! \mathcal{E}_0^{2n+2}} |\mathcal{E}(t)|^{2n-2} \exp \left\{ -\frac{|\mathcal{E}(t)|^2}{\mathcal{E}_0^2} \right\} \\ \times \{ n^2 \mathcal{E}_0^4 + |\mathcal{E}(t)|^2 [-2n\mathcal{E}_0^2 + |\mathcal{E}(t)|^2] \}, \quad (9)$$

$J_{nn;10}(t) = J_{nn;01}^*(t)$, $\mathcal{E}_0 = \sqrt{2m\omega_0\hbar}$, and

$$\mathcal{E}(t) = E_-^2(t) + 2 \cos(\omega_0 t) E_-(t) E_+(t) + E_+^2(t) \quad (10)$$

$$= \int_{-\infty}^t ds \exp(-is\omega_0) E(s). \quad (11)$$

For later convenience, we have defined $E_+(t) = \int_{-\infty}^t ds E(s) G_+(t-s) / G_+(t)$, and $E_-(t) = \int_{-\infty}^t ds E(s) G_-(s) / G_-(t)$, where $G_{\pm}(s)$ denotes the inverse Laplace transform of $\hat{G}_{\pm}(z) = (z^2 + \omega_0^2)^{-1}$. The specific combination of $E_+(t)$ and $E_-(t)$ in Eq. (10) is responsible for the simple result in Eq. (11). As shown below, this precise form is lost in the open system case giving rise to phase control. In the following, we use linearly chirped laser pulses

$$E(t) = E_0 e^{-4\left(\frac{t-t_0}{\Delta t}\right)^2} \cos [\Omega_L(t-t_0) + \chi(t-t_0)^2], \quad (12)$$

where t_0 and Δt are the center and width of the Gaussian pulse envelope, E_0 and Ω_L are the field strength and carrier frequency of the laser with chirp rate χ . Changing the sign of χ causes a change in the laser phase while retaining the intensity profile.

In the long time regime, $t \rightarrow \infty$, $\mathcal{E}(t)$ becomes the Fourier transform of the field $E(t)$. This implies that the term $|\mathcal{E}(t)|$ does not contain any information about the spectral phase.

Hence, here, laser phase information is not encoded in either $J_{nn;00}(t)$ or $J_{nn;11}(t)$, but only in $J_{nn;01}(t)$. Thus, if the initial state is an incoherent superposition of $|0\rangle$ and $|1\rangle$ then the expectation value of \hat{O} does not depend on the phase function $\varphi(\omega)$. This result makes no reference to the field strength, but is a particularity of the chosen system which is not expected to be true in general.

In order to make a connection with the general weak field results derived in Refs. 12 and 17, we consider Eqs. (7)-(9) in the weak field regime, $\sqrt{|S(\omega_0)|}/\mathcal{E}_0 \ll 1$, to get:

$$J_{00;00}(\infty) = 1 - J_{00;11}(\infty), \quad (13)$$

$$J_{00;10}(\infty) = \frac{1}{\mathcal{E}_0} \int_{-\infty}^{\infty} ds e^{-i\omega_0 s} E(s), \quad (14)$$

$$J_{00;11}(\infty) = \frac{1}{\mathcal{E}_0^2} \left| \int_{-\infty}^{\infty} ds e^{-i\omega_0 s} E(s) \right|^2. \quad (15)$$

These expressions correspond to the typical results in lowest order perturbation theory in the field amplitude²⁹. Clearly, phase dependence is not manifest in the long-time diagonal terms $J_{00;00}(\infty)$ or $J_{00;11}(\infty)$. Sample results are shown in Fig. 1, it is clear that no phase dependence is present after the pulse is over. Hence, the long time regime is defined as *after* the pulse is over. As discussed below, this is no longer the case when environmental effects are considered.

Interestingly, for this particular case, the weak field condition $\sqrt{|S(\omega_0)|}/\mathcal{E}_0 = \sqrt{|S(\omega_0)|}/\sqrt{2m\hbar\omega_0} \ll 1$ implies that, for the same value of $\sqrt{|S(\omega_0)|}$, one could be in a weak or strong field regime depending on the coupling constant ($k = m\omega_0^2$) and on the mean level spacing $\hbar\omega_0$.

IV. NON-UNITARY EVOLUTION AND ONE-PHOTON PHASE-CONTROL

Consider then the case of dynamics and control in an open system. We treat the dissipative dynamics using the influence functional approach³⁰. The starting condition is obtained by coupling the central system S to an external system B which is represented by an infinite number of freedoms³⁰. This system B can be, e.g., a thermal bath, the vibrational modes of a molecular complex, blackbody radiation, etc. The Hamiltonian of the the system S plus B

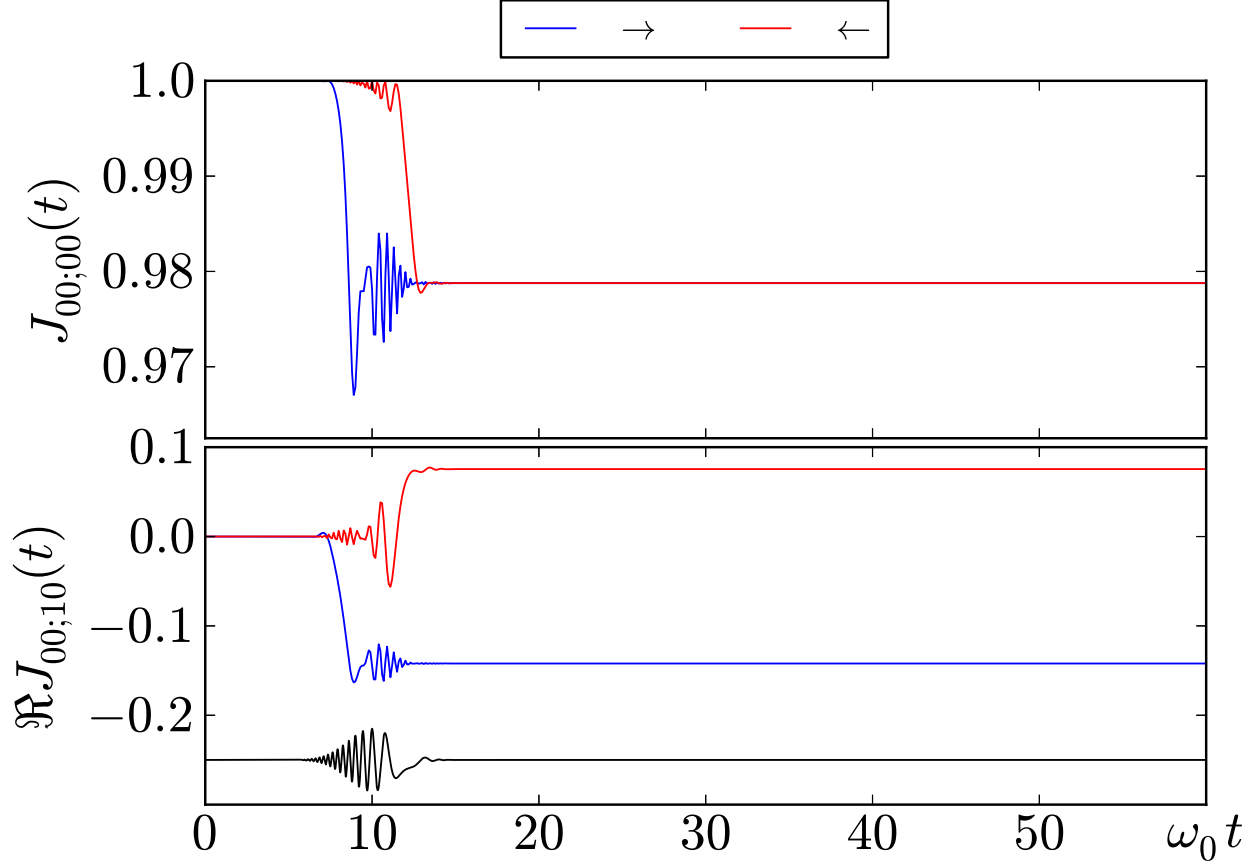


FIG. 1. **Phase dependence in unitary dynamics.** $J_{00;00}(t)$ (upper panel) and $J_{00;10}(t)$ (lower panel) induced by the chirped pulse in Eq. (12) with $\omega_0 t_0 = 10$, $\Omega_L = 10\omega_0$, $\Delta t\omega_0 = 4$ and $\sqrt{|S(\omega_0)|}/\mathcal{E}_0 = 0.003415$ with $\chi = 2.5$ [(\rightarrow) dark blue curve] and $\chi = -2.5$ [(\leftarrow) light red curve]. For reference, we have added at the bottom of the lower panel the laser pulse as a function of time (black curve).

can be written as

$$\hat{H} = \hat{H}_S + \hat{H}_B + \hat{H}_{SB} + \hat{V}_L \quad (16)$$

where $\hat{H}_S + \hat{V}_L$ are given in Eq. (4), \hat{H}_B is the Hamiltonian of the thermal bath and \hat{H}_{SB} describes the interaction of the system with B. We assume that system B is composed of a collection of harmonic oscillators with masses m_j , frequencies ω_j and coupled linearly to S with constant couplings c_j ^{31–33}.

After tracing over the environment the influence of the bath on the time evolution of the system S is described via the spectral density $J(\omega)$, given by^{31–33} $J(\omega) = \pi \sum_{j=1}^{\infty} \frac{c_j^2}{2m_j\omega_j} \delta(\omega - \omega_j)$. Once $J(\omega)$ is fixed, one can express the relaxation process by means of the dissipative kernel $\gamma(s) = \frac{2}{m} \int_0^{\infty} \frac{d\omega}{\pi} \frac{J(\omega)}{\omega} \cos(\omega s)$, while the decoherence process induced by thermal fluctuations

can be described by the decoherence kernel $K'(s) = \int_0^\infty \frac{d\omega}{\pi} J(\omega) \coth\left(\frac{\hbar\beta\omega}{2}\right) \cos(\omega s)$. Here $\beta = 1/k_B T$ and T denotes the temperature of the thermal bath.

Below, we primarily employ the most commonly used spectral density, the Ohmic spectral density with a finite Drude cutoff ω_D ,

$$J_{\text{Ohm}}(\omega) = m\gamma\omega\omega_D^2 / (\omega^2 + \omega_D^2), \quad (17)$$

where γ is the strength coupling constant to the thermal bath. This spectral density generates the dissipative kernel $\gamma(s) = \gamma\omega_D \exp(-\omega_D|t|)$. In the limit when the cutoff frequency ω_D tends to infinity, $\gamma(s) \rightarrow 2\gamma\delta(s)$, corresponding to Ohmic dissipation.

A. Description of the Initial State

Often, the initial state of S + B is assumed to be uncorrelated product^{30,31}, i.e. $\hat{\rho}_{S+B} = \hat{\rho}_S \otimes \hat{\rho}_B$. However, this is not a sensible approximation³² since it implies that system-bath interaction is turned on suddenly when the observation begins. In the absence of a specific initial system preparation, the most likely initial state for S+B is thermal. In this case if the coupling to the environment is strong, then the equilibrium state is given by³² $\hat{\rho}_{S,\beta} = Z_\beta^{-1} \text{tr}_B \exp\left[-\left(\hat{H}_S + \hat{H}_B + \hat{H}_{SB}\right)\beta\right]$, where Z_β is the total partition function and tr_B denotes a trace over the bath.

For our particular case, $\hat{\rho}_{S,\beta}$ can be expressed analytically in terms of the effective Hamiltonian^{19,34,35} $\hat{H}_{\text{eff}} = \frac{1}{2m_{\text{eff}}}\hat{p}^2 + \frac{1}{2}m_{\text{eff}}\omega_{\text{eff}}^2\hat{q}^2$, with effective mass $m_{\text{eff}} = \omega_{\text{eff}}^{-1} \sqrt{\langle p^2 \rangle \langle q^2 \rangle^{-1}}$, and effective frequency $\omega_{\text{eff}} = 2(\hbar\beta_{\text{TB}})^{-1} \text{arccoth}\left(\frac{2}{\hbar} \sqrt{\langle p^2 \rangle \langle q^2 \rangle}\right)$, being $\langle q^2 \rangle = \text{tr}_S(\hat{q}^2 \hat{\rho}_{S,\beta})$ and $\langle p^2 \rangle = \text{tr}_S(\hat{p}^2 \hat{\rho}_{S,\beta})$, the equilibrium second moments^{32,34}. This \hat{H}_{eff} definition allows us to express $\hat{\rho}_{S,\beta}$ as

$$\hat{\rho}_{S,\beta} = Z_\beta^{-1} \sum_{n=0}^{\infty} \exp(-E_{n_\beta} \beta_{\text{TB}}) |n_\beta\rangle \langle n_\beta|, \quad (18)$$

where $\{E_{n_\beta} = \hbar\omega_{\text{eff}}(n + \frac{1}{2})\}$ are the eigenvalues and $\{|n_\beta\rangle\}$ the eigenstates of the effective Hamiltonian \hat{H}_{eff} . At high temperature, $\hbar\omega_0\beta \ll 1$ and $\frac{1}{2}\hbar\gamma\beta \ll 1$, m_{eff} and ω_{eff} approach their bare values m and ω_0 , respectively and, therefore, $\hat{\rho}_{S,\beta}$ approaches the canonical distribution^{19,34,36}. By contrast, at low temperatures $\hbar\omega_0\beta \gg 1$ and $\frac{1}{2}\hbar\gamma\beta \gg 1$, m_{eff} and ω_{eff} deviate from the bare values m and ω_0 due to damping^{19,34,36}. This deviation from the

canonical distribution implies that the initial equilibrium state [Eq. (18)] contains stationary off-diagonal elements when it is projected on the eigenbasis of \hat{H}_S . Note further that these off-diagonal elements are expected to vanish in classical mechanics³⁷. Hence, the existence of these terms is a purely quantum mechanical.

In order to explore the strength of the off-diagonal elements introduced in Eq. (18), we show, in Fig. 2, the matrix element $\langle 0|\hat{\rho}_{S,\beta}|2\rangle$ as a function of the coupling constant γ and temperature T for the non-Markovian regime, $\omega_D = \omega_0$ (upper panel) and for the Markovian regime, $\omega_D = 100\omega_0$ (lower panel). In both cases, for fixed γ the matrix element $\langle 0|\hat{\rho}_{S,\beta}|2\rangle$ is larger at low temperatures, whereas for fixed temperature it is larger for larger coupling constant γ . From Fig. (2) one can also see that the larger the cutoff ω_D , the larger the matrix element $\langle 0|\hat{\rho}_{S,\beta}|2\rangle$ at fixed γ and T . This is consistent with the fact that the more Markovian the system, the larger is the decay rate, and therefore the larger the *effective* coupling to the bath (for an extended discussion on this parameter dependence see Ref. 19).

Note that increasing the value of $\langle 0|\hat{\rho}_{S,\beta}|2\rangle$ would imply a stronger contribution of these off-diagonal terms to the subsequent dynamics. However, in general, it would also imply fast relaxation, and therefore very fast loss of phase information. That is, coupling of the system to the bath plays two roles in phase control, one to enhance the phase control and one to cause relaxation. Below, in order to explicitly explore the system time-evolution and elucidate the contributions to phase control, we choose a moderate coupling constant, $\gamma = 0.1\omega_0$ and low temperature $\hbar\omega_0/k_B T = 40$.

B. Effect of the Initial Correlations

Based on the discussion for the unitary case, one can identify the deviations from the canonical distribution, and the related presence of off-diagonal elements in the initial density matrix, as the first contribution of the bath to one photon phase control. This implies that when laser excitation takes place, it finds *off-diagonal* elements of $\hat{\rho}_S$, where laser phase information could be encoded (see below). This contribution occurs then on the time scale of the laser field¹⁷.

Before considering the time evolution of the off-diagonal elements, it is useful to consider which of these terms are non-zero. From the symmetry of the resulting equilibrium state [see Eq. (18)], we expect the non-vanishing off-diagonal elements $\langle n|\hat{\rho}_{S,\beta}(0)|m\rangle$ that satisfy:

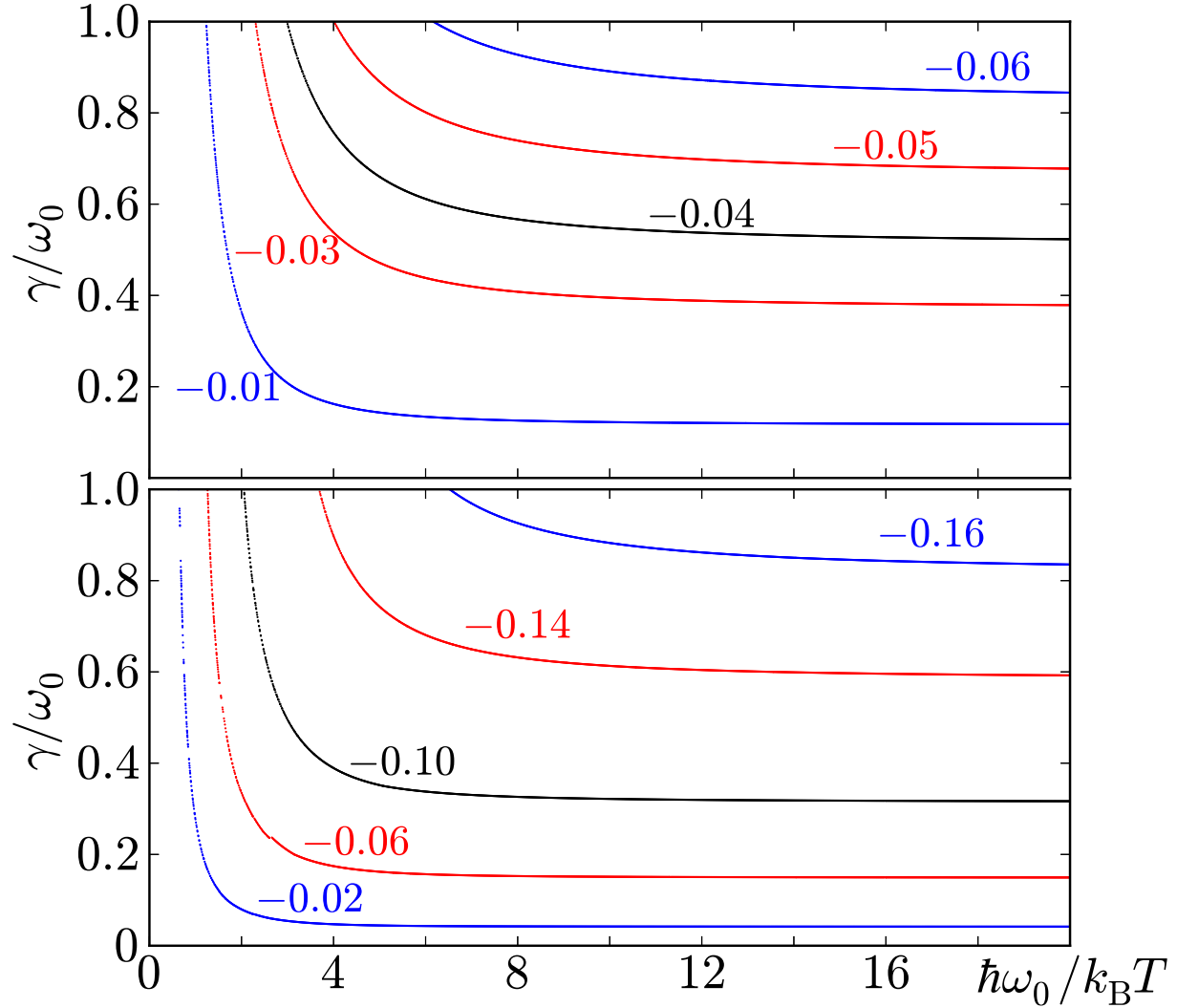


FIG. 2. **Stationary coherence generated by the Ohmic spectral density.** Contours of constant matrix element $\langle 0|\hat{\rho}_{S,\beta}|2\rangle$ as a function of γ and T for fixed $\omega_D = \omega_0$ (upper panel) and for $\omega_D = 100\omega_0$ (lower panel).

parity($\langle n|q\rangle$) \times parity($\langle q|m\rangle$) = even; this is the case in, e.g., $\langle 0|\hat{\rho}_{S,\beta}(0)|2\rangle$ or $\langle 1|\hat{\rho}_{S,\beta}(0)|3\rangle$. Hence, the bath is not able to induce stationary off-diagonal elements such as $\langle 0|\hat{\rho}_{S,\beta}(0)|1\rangle$ or $\langle 1|\hat{\rho}_{S,\beta}(0)|2\rangle$. Although a formal analysis of this fact could be carried out on the basis of the transitions induced by the bath after being traced out, for our purposes it suffices to consider this result as a consequence of the symmetries of the equilibrium state. Note that a similar analysis needs to be carried out for each particular system.

To demonstrate the phase dependence due to the stationary coherences in our model system, consider the propagating function element responsible for the $\langle 0|\hat{\rho}_S(0)|2\rangle = \langle 0|\hat{\rho}_{S,\beta}|2\rangle$

to the time-evolution of the ground state $\langle 0|\hat{\rho}_S(t)|0\rangle$,

$$J_{00;20}(t) = \sqrt{\frac{8\pi^2}{q_0^8 \hbar^4 \det \mathbf{M}}} \frac{1}{N(t)} e^{\frac{1}{2} \mathbf{E}^T \mathbf{A} \mathbf{E}} \left\{ (\mathbf{A}_{33} - q_0^2) \hbar^2 \right. \\ \left. - 2 [(\mathbf{A}_{13} - \mathbf{A}_{23}) E_-(t) (\mathbf{A}_{33} - \mathbf{A}_{34})]^2 E_+(t) \right\}, \quad (19)$$

where $q_0 = \sqrt{\hbar/m\omega_0}$, $N(t) = 2\pi\hbar \frac{1}{m} |G_+(t)| \sqrt{2\pi \langle \hat{q}^2 \rangle}$, and $\mathbf{E} = (E_+(t), E_-(t))$ with $E_+(t) = \int_0^t ds E(s) G_+(t-s)/G_+(t)$, $E_-(t) = \int_0^t ds E(s) G_-(s)/G_-(t)$. Here $G_+(s)$ denotes the inverse Laplace transform of $G(z) = (z^2 + z\gamma(z) + \omega_0^2)^{-1}$, being $\gamma(z)$ the Laplace transform of the dissipative kernel $\gamma(s)$ ³². $G_-(s)$ is related to $G_+(s)$ by means of the relation $\frac{G_-(s)}{G_-(t)} = \dot{G}_+(t-s) - \frac{G_+(t-s)}{G_+(t)} \dot{G}_+(s)$. As required, in the limit of vanishing coupling to the bath $\gamma \rightarrow 0$, $G_+(s) = G_-(s) = \frac{1}{2i\omega_0} [\exp(\lambda_1 t) - \exp(\lambda_2 t)]$ with $\lambda_{1,2} = \pm i\omega_0$ and $\mathbf{E}^T \mathbf{A} \mathbf{E} = -2|\mathcal{E}(t)|^2/\mathcal{E}_0^2$, the expressions in Eqs. (7-9) are recovered. In Appendix A, we present the explicit expressions for \mathbf{A} and \mathbf{M} ³⁸.

In the long time regime,

$$J_{00;20}(t) \sim \frac{\hbar^3 (\langle p^2 \rangle - m\omega_0 \hbar) A^2(t) E_-^2(t)}{m^2 \langle q^2 \rangle \dot{A}^2(t) \sqrt{2m\omega_0 (4m\omega_0 \langle q^2 \rangle - \hbar)}} \\ \times \frac{\exp(\frac{1}{2} \mathbf{E}^T \mathbf{A} \mathbf{E})}{\sqrt{4m^4 \langle q^2 \rangle \frac{\dot{A}^2(t)}{G_+^2(t)} + \hbar^2 (\langle p^2 \rangle - m\omega_0 \hbar)}}, \quad (20)$$

with

$$\mathbf{E}^T \mathbf{A} \mathbf{E} \sim -\frac{2E_-^2(t)}{m\omega_0 \hbar - \langle p^2 \rangle - m^2 \frac{\dot{A}^2(t)}{A^2(t)} \langle q^2 \rangle}, \quad (21)$$

where $A(t)$ is the antisymmetric correlation function $A(t) = \frac{1}{2i} \langle \hat{q}(t) \hat{q} - \hat{q} \hat{q}(t) \rangle = -\frac{\hbar}{2m} G_+(t)$ (see Appendix A). In contrast to the result in Eq. (10), Eq. (21) is independent of $E_+(t)$; this is a result of the time-symmetry breaking anticipated above. Hence, it is clear that in this case, $\mathbf{E}^T \mathbf{A} \mathbf{E}$ differs from the squared modulus of the Fourier transform and therefore phase information can be stored, *even* in the diagonal elements of the propagating function.

This being the case, the spectral phase information contained in the propagating functions element $J_{00;20}$ can now affect the dynamics of the expectation value in Eq. (3). Figure 3 shows $J_{00;20}$ as a function of time for $\chi = 2.5$ (continuous blue, dashed black and dotted cyan

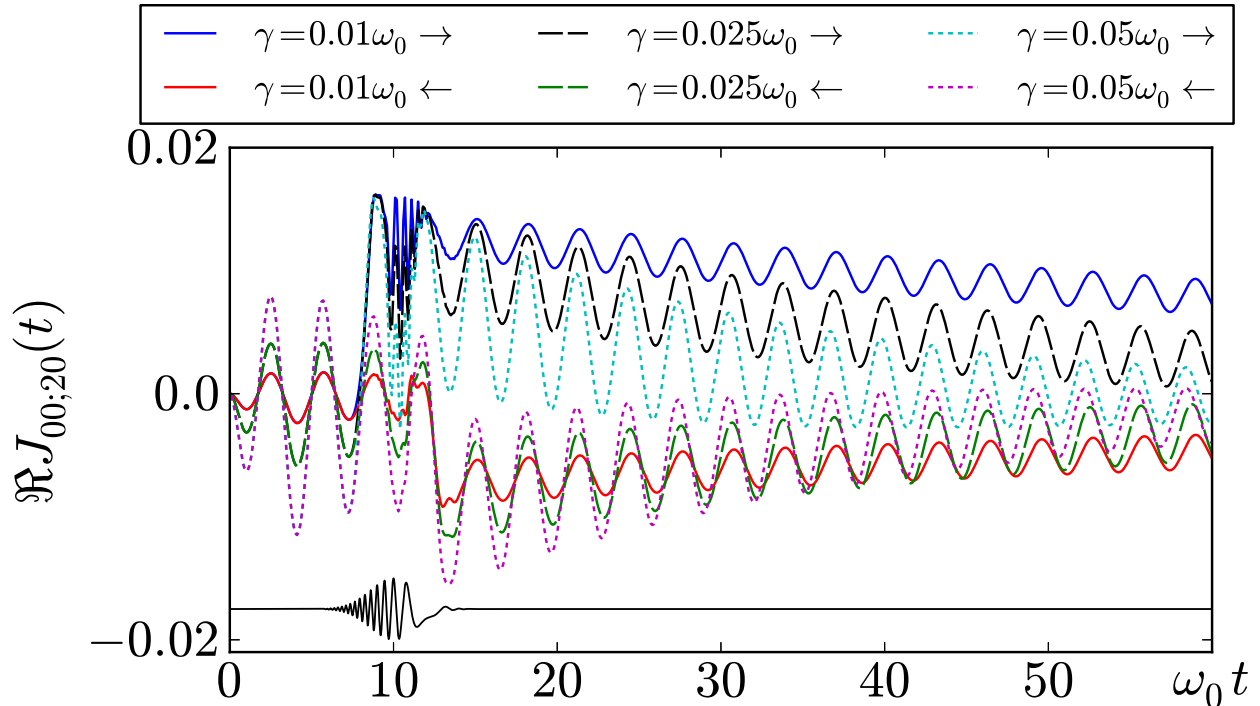


FIG. 3. **Time evolution of the propagating function elements associated with stationary coherences.** $J_{00;20}(t)$ induced by the chirped pulse in Eq. (12) with $\omega_D = \omega_0$ and $\hbar\omega_0/k_B T = 40$. Here $\omega_0 t_0 = 10$, $\Omega_L = 10\omega_0$, $\Delta t\omega_0 = 4$ and $\sqrt{|S(\omega_0)|}/\mathcal{E}_0 = 0.003415$ with $\chi = 2.5$ [(\rightarrow) continuous blue, dashed black and dotted cyan curves] and $\chi = -2.5$ [(\leftarrow) continuous red, dashed green and dotted magenta curves] for various values of the coupling constant γ .

curves) and $\chi = -2.5$ (continuous red, dashed green and dotted magenta curves) and for three different values of the coupling constant $\gamma = 0.01\omega_0$, $\gamma = 0.025\omega_0$ and $\gamma = 0.05\omega_0$.

Remarkably, in Fig. 3, $J_{00;20}(t)$ shows a time dependence *before* the laser excitation occurs, resulting from the time dependence of the antisymmetric correlation function $A(t)$. This is a manifestation of an *an incoherent flux at equilibrium* between eigenstates. The detailed origin of this incoherent flux is well beyond the scope of this work and will be discussed elsewhere.

C. Effect of Time-reversal-symmetry Breaking

The discussion above focused upon stationary features of non-unitary evolution that assist OPPC. Here we consider dynamical features (time-reversal-symmetry breaking) in non-unitary evolution that enhance OPPC. For this propose it suffices to study one of the

propagating function elements. For example, the $J_{00;00}(t)$ element reads

$$J_{00;00}(t) = \sqrt{\frac{1}{q_0^4} \frac{2^4}{\det \mathbf{M}} \frac{1}{N(t)}} \exp\left(\frac{1}{2} \mathbf{E}^T \mathbf{A} \mathbf{E}\right), \quad (22)$$

Based on Eq. (21), it is clear that the propagating element $J_{00;00}(t)$ depends on the electric field phase in the long time regime for the open system case, thus allowing for the encoding of phase information.

Fig. 4 shows $J_{00;00}(t)$ using the same parameters as in Fig. 3. For the unitary case

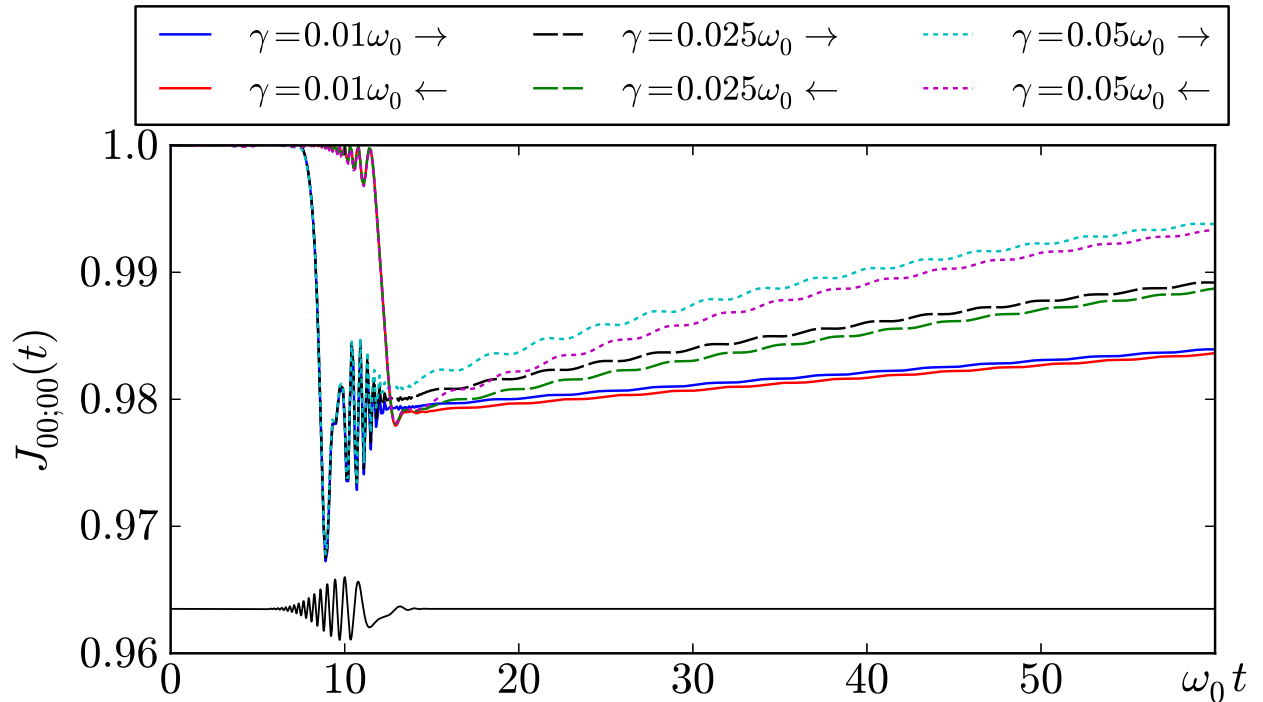


FIG. 4. **Time evolution of the propagating function elements associated to populations.** $J_{00;00}(t)$ induced by the chirped pulse in Eq. (12). Parameter values as in Fig. 3.

[see Fig. 1], after the pulse is over there is no phase information in $J_{00;00}(t)$. However, for the non-unitary dynamics the effect of the phase persists in the long time regime, albeit diminished by the underlying incoherent thermal process. Further, the magnitude of the phase effect in $J_{00;00}(t)$, for short times after the pulse is over, is larger for the larger values of the coupling to the environment. However, in the long time regime, due to the equilibration, the phase information is lost.

D. Control of Observables

Consider then, as an example, control over the population of the n -th system eigenstate, e.g., the population of the ground state, with $\hat{O} = |0\rangle\langle 0|$. Under unitary dynamics, and for an incoherent initial state, the time evolution of the ground state population is completely generated by the propagating function element $J_{00,00}(t)$ (see Fig. 1), and, as described above, no phase control is possible.

The situation is different in the presence of an environment. The upper panel of Fig. 5 shows the time evolution of the ground state population $\langle 0|\hat{\rho}_S(t)|0\rangle$ using the same parameters as in Fig. 3. Here phase dependence of a quantity that commutes with the bare Hamiltonian \hat{H}_S , is evident. Note that the full pulse effectively spans a time of $10\omega_0^{-1}$. Hence, although phase control must be lost over long times due to the environmental coupling, the control still survives over an extended time after the pulse is over, i.e., in a “non-equilibrated regime”.

The lower panel of Fig. 5 shows the time-evolution dynamics of the first excited state $\langle 1|\hat{\rho}(t)|1\rangle$. The characteristics of the phase dependence are similar to those for the ground state dynamics, the smaller phase amplitude and slower decay being the only noticeable differences. This arises from the very small initial population in $\langle 1|\hat{\rho}_S(t)|1\rangle$ (0.000446 for $\gamma = 0.01\omega_0$, 0.00113 for $\gamma = 0.025\omega_0$ and 0.00223 for $\gamma = 0.05\omega_0$) and the fact that for the times where the amplitude of the phase dependence is moderate, immediately after the pulse, the propagating elements $J_{11;\nu\mu}$ are small. In particular, the term responsible for the transfer of population from the ground state, $J_{11;00}$, behaves as $\sim \frac{1}{2}\mathbf{E}^T\mathbf{A}\mathbf{E} \exp\left(\frac{1}{2}\mathbf{E}^T\mathbf{A}\mathbf{E}\right)$ whereas $J_{00;00}$ behaves as $\sim \exp\left(\frac{1}{2}\mathbf{E}^T\mathbf{A}\mathbf{E}\right)$ [see Eq. (22)].

In both panels of Fig. 5 one observes that, after the pulse is over, the state populations reach certain chirp-dependent values and then relax. Comparing the results in Fig. 5 with the time evolution of the $J_{00;00}$ element in Fig. 4, shows that the phase dependence, for this set of parameters, is primarily dictated by $J_{00;00}$, with no appreciable influence from the stationary coherence $\langle 0|\hat{\rho}_S(0)|2\rangle$. This is a result of the small value of $J_{00;20}(t)\langle 0|\hat{\rho}_{S,\beta}|2\rangle$, which is the leading off-diagonal-contribution to the dynamics of $\langle 0|\hat{\rho}_S(0)|0\rangle$. In particular, for $\gamma = 0.01\omega_0$ we have that $\langle 0|\hat{\rho}_{S,\beta}|2\rangle = -0.00088$; while for $\gamma = 0.025\omega_0$ and $\gamma = 0.05\omega_0$, we have that $\langle 0|\hat{\rho}_{S,\beta}|2\rangle = -0.00219$ and $\langle 0|\hat{\rho}_{S,\beta}|2\rangle = -0.00435$, respectively. The off-diagonal element contribution may well be larger for other kinds of systems and couplings.

Given our goal of significant phase control, Fig. 2 suggests that we increase, e.g., the ratio

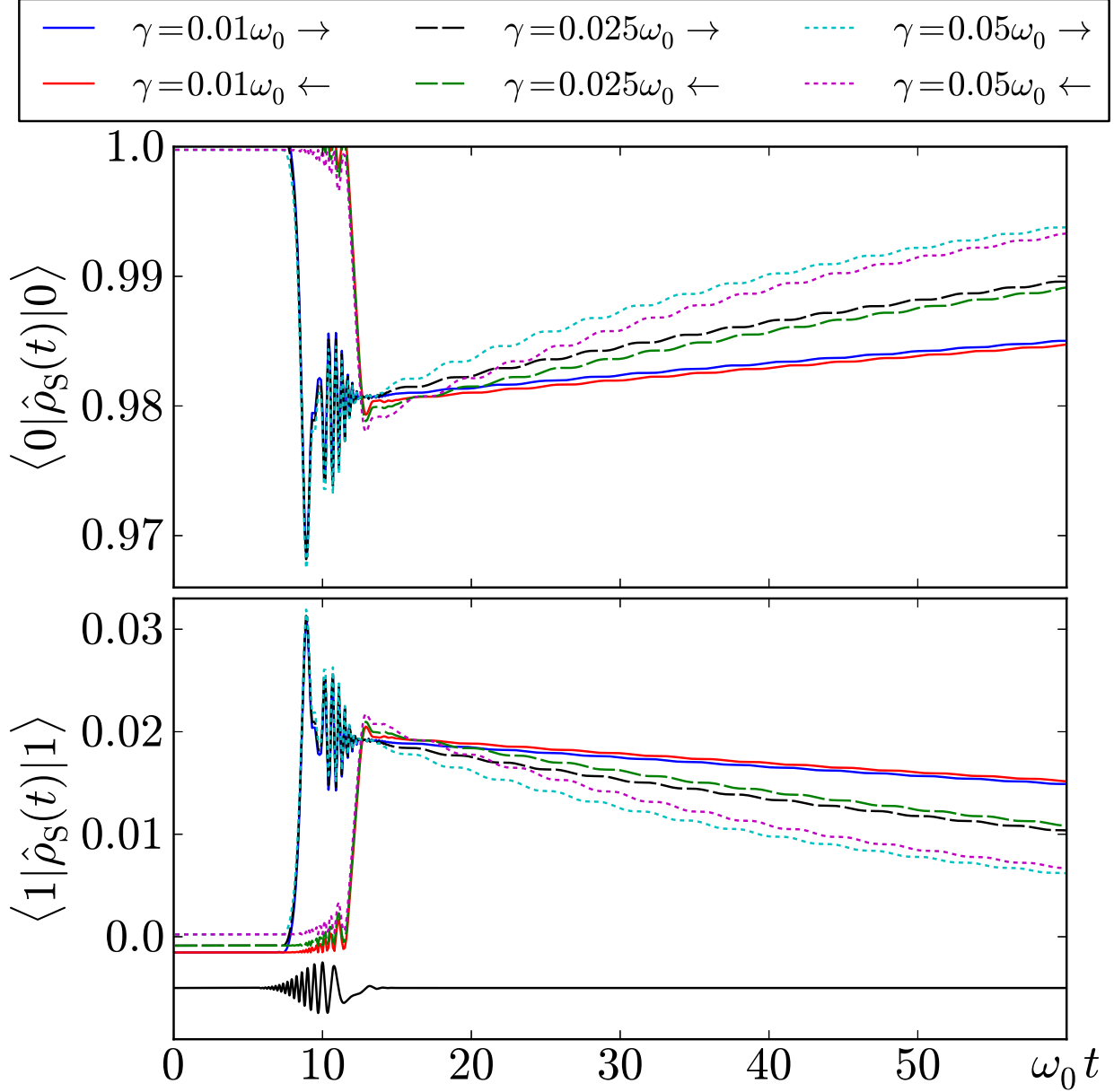


FIG. 5. **Influence of the coupling constant for the Ohmic spectral density.** Time evolution of $\langle 0 | \hat{\rho}(t) | 0 \rangle$ (upper panel) and $\langle 1 | \hat{\rho}(t) | 1 \rangle$ (lower panel) induced by the chirped pulse in Eq. (12). Parameter values as in Fig. 3.

γ/ω_0 . However, doing so would also induce faster decay rates, and the phase dependence would quickly vanish. Alternately, since the thermal energy at room temperature is $\sim 1/40$ eV and energy of the optical transitions are between 1.6 to 3.4 eV, increasing the ratio $\hbar\omega_0/k_B T$ could be a more promising alternative to enhance control. However, as seen from Fig. 2, for $\hbar\omega_0/k_B T > 10$, $\langle 0 | \hat{\rho}_\beta | 2 \rangle$ becomes basically temperature-independent. Thus environmentally assisted phase control has the fundamental challenge that the terms that assist control also

induce, simultaneously, equilibration with the bath.

E. Influence of the Non-Markovian Character of the Dynamics

In general, open quantum systems undergo non-Markovian provide that the spectrum of the thermal fluctuations is not flat (coloured noise³⁹). Formally, the Markovian regime is reached when the spectral density has a linear monotonic behaviour and thermal energy $k_B T$ is the larger energy scale of the system. For the Ohmic spectral density in Eq. (17), increasing ω_D is known to bring the system closer to the Markovian limit. To examine the non-Markovian effects we show, in Fig. 6, the time evolution of the ground state and first excited state, generated by the laser pulse for different values of the cutoff frequency ω_D . The amplitude of the phase effect, for short times after the pulse is over, is seen to be larger for the Markovian cases ($\omega_D = 10\omega_0$ and $\omega_D = 100\omega_0$) than for the non-Markovian case ($\omega_D = \omega_0$). This reflects the stronger effective system-bath coupling in the Markovian case¹⁹. As a consequence, the time reversibility of the unitary dynamics is lost more effectively in the non-Markovian case. However, in the long time regime the non-Markovian dynamics, due to its weaker effective coupling to the bath, has a larger phase-effect, albeit the overall phase control is very small.

F. Effect of the a Different Spectral Density

Although the main lines of the above discussion are general and intuitive, the numerical results above pertain to the Ohmic spectral density [17]. Motivated by our recent observation⁴⁰ that the effect of the vibrations and the solvent— in systems such as dye molecules, amino acid proteins and some photochemical systems (e.g., rhodopsin and green fluorescence proteins)— could be effectively described by a sub-Ohmic spectral density; we consider this alternate spectral density below. Note that sub-Ohmic spectral densities are characterized by slow decay rates, even in the strong coupling regime⁴⁰. Hence, this spectral density may well be of some interest in terms of phase-control, where it may result in a prolonged phase-control effect.

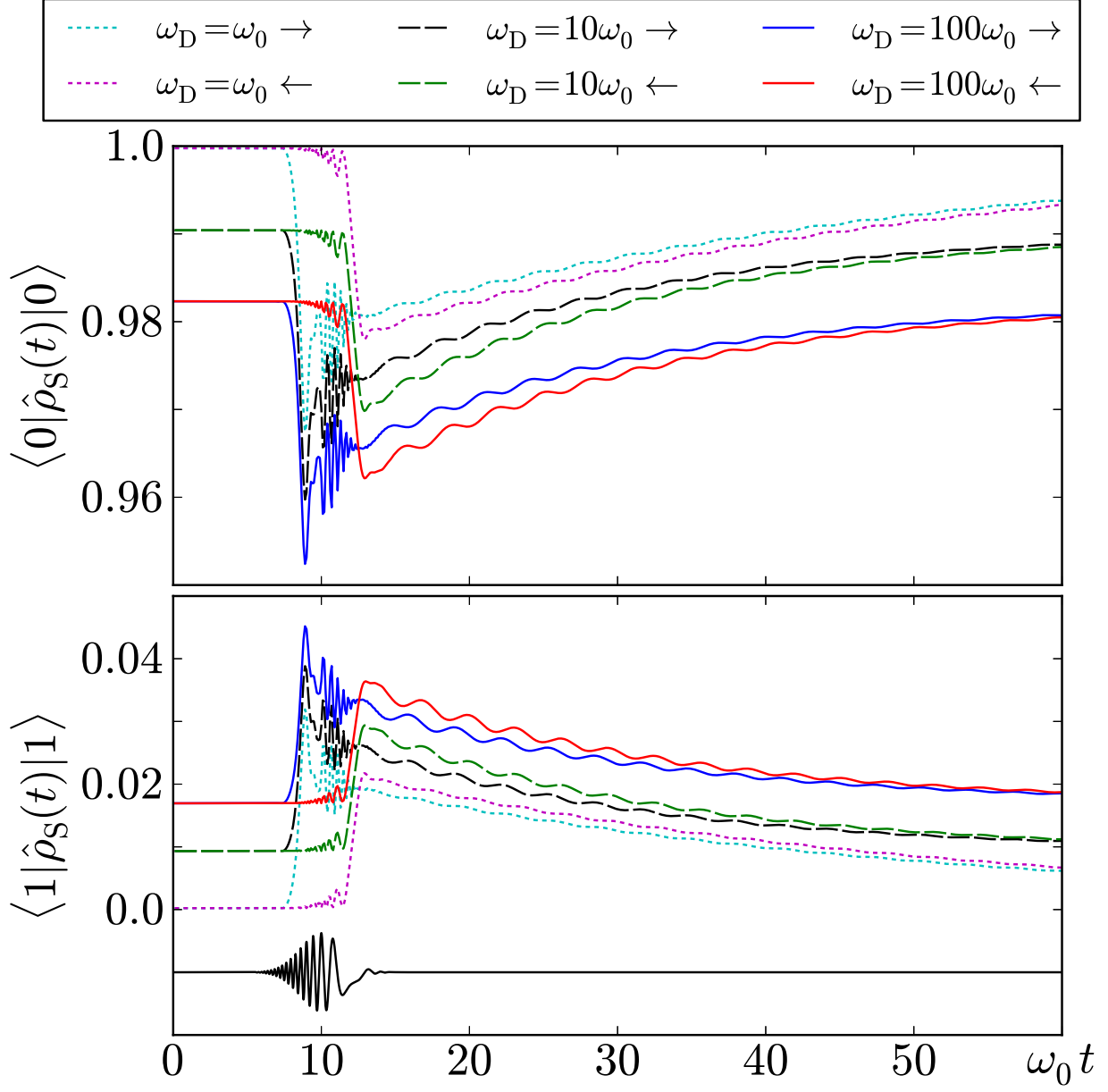


FIG. 6. **Influence of the non-Markovian character of the dynamics.** Time evolution of $\langle 0|\hat{\rho}_S(t)|0\rangle$ (upper panel) and $\langle 1|\hat{\rho}_S(t)|1\rangle$ (lower panel) with $\gamma = 0.05\omega_0$ and $\hbar\omega_0/k_B T = 40$ for different values of the cutoff frequency ω_D . The value of the laser parameters are as in Fig. 3.

The sub-Ohmic spectral density with exponential decay is given by

$$J_{\text{sOhm}}(\omega) = m\gamma\omega_{\text{ph}}^{1-s}\omega^s \exp(-\omega/\omega_D), \quad (23)$$

with $0 < s < 1$, and ω_{ph} is an auxiliary phononic scale frequency. For this case the relevant coupling constant is $\gamma\omega_{\text{ph}}^{1-s}$ and the spectral density generates the dissipative kernel

$\gamma(s) = \frac{4}{\pi} (1 + t^2 \omega_D^2)^{-s/2} \omega_{\text{ph}}^{1-s} \Gamma(s) \cos[s \arctan(\omega_D t)]$. In the limit where $\omega_D \rightarrow \infty$, $\gamma(t) \rightarrow \frac{4}{\pi} t^{-s} \omega_{\text{ph}}^{1-s} \Gamma(s) \cos(\frac{\pi}{2}s)$ which, by contrast to the Ohmic case, also leads to non-Markovian effects. In the short time regime, $\omega_D t \ll 1$, $\gamma(t)/\gamma(0) \sim 1 - \frac{1}{2}s(1+s)(\omega_D t)^2$, which resembles the functional form of a Gaussian decay at short times. In the long time regime, $\omega_D t \gg 1$, $\gamma(t)/\gamma(0) \sim \cos(\frac{\pi}{2}s)(\omega_D t)^{-s}$, so that the long time decay is only algebraic, $1/t^s$.

Fig. 7 shows the sub-Ohmic analog of the Ohmic calculation in the upper panel in Fig. 2, where values of the stationary off-diagonal element $\langle 0|\hat{\rho}_{S,\beta}|2\rangle$, larger than in the Ohmic case, are seen. Figure 8 shows the time evolution of the ground and first excited states, where

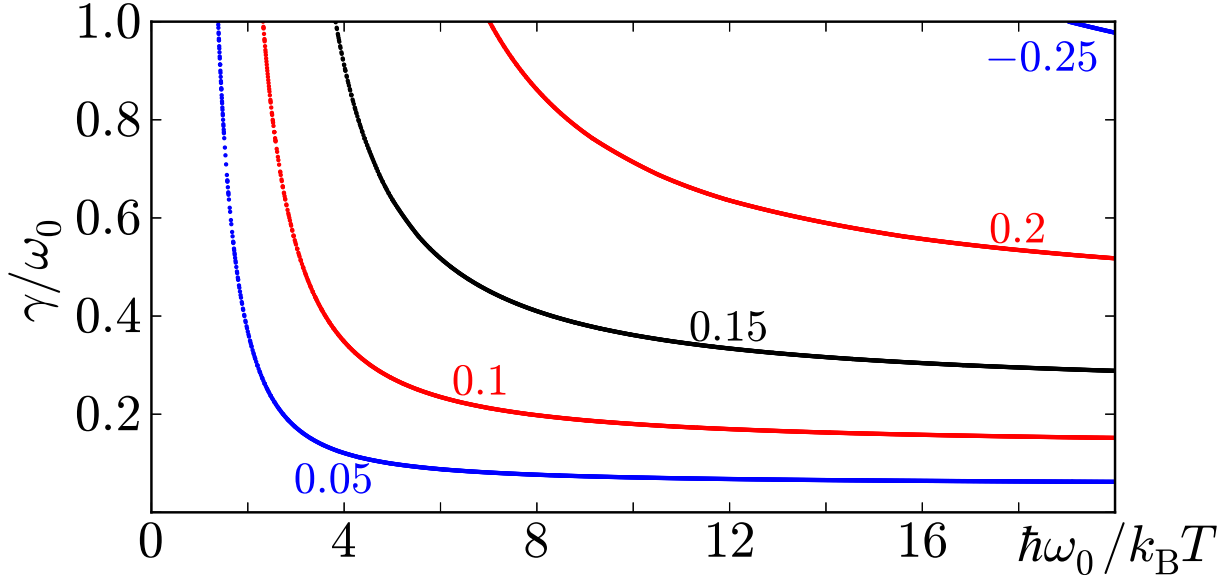


FIG. 7. **Stationary coherence generated by the sub-Ohmic spectral density.** Contours of constant matrix element $\langle 0|\hat{\rho}_{S,\beta}|2\rangle$ as a function of γ and T for fixed $\omega_{\text{ph}} = \omega_0$, $\omega_D = \omega_0$ and $s = 0.1$.

the system-bath interaction is described by a sub-Ohmic spectral density [23] and where the parameters are the same as those in Fig. 5. The new feature seen here is the persistence of population oscillations in the ground state which is also present, although to lesser extent, in the first excited state. This observation is consistent with the recent finding that sub-Ohmic spectral densities are able to maintain coherent oscillations for longer times in the spin-boson model⁴¹.

One further feature occurs at short times where, the phase amplitude is slightly larger in the sub-Ohmic case than in the Ohmic case. However, due to the Gaussian-like decay discussed above, this larger phase dependence decays faster here than in the Ohmic case (where for short times, the decay is exponential). However, this fast relaxation is compensated

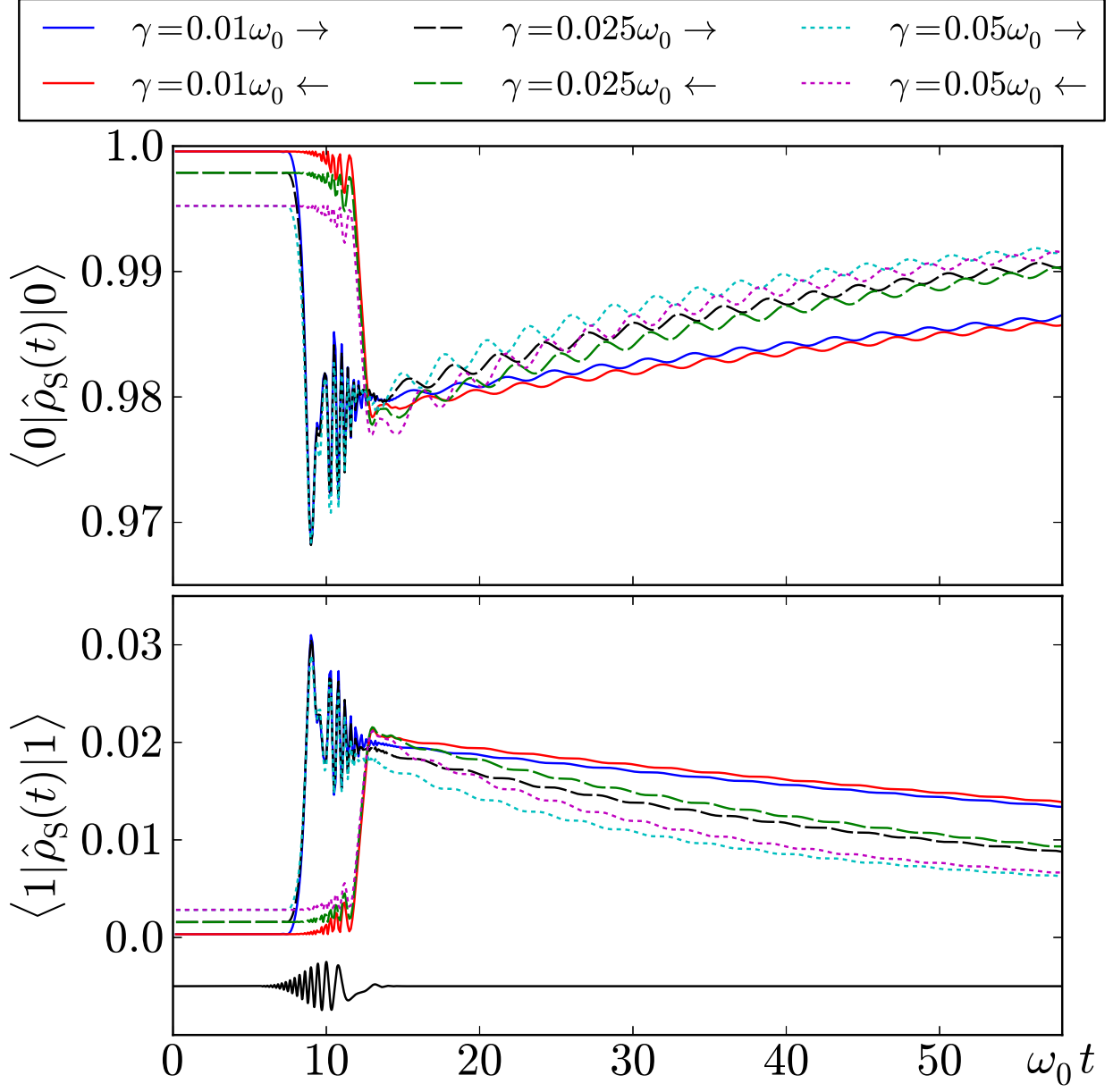


FIG. 8. **Influence of the coupling constant for the sub-Ohmic spectral density.** Time evolution of $\langle 0 | \hat{\rho}_S | 0 \rangle$ induced by the chirped pulse in Eq. (12). with and $\hbar\omega_0/k_B T = 40$, $\omega_{\text{ph}} = \omega_0$, $\omega_{\text{D}} = \omega_0$ and $s = 0.1$. The value of the laser parameters are as in Fig. 3.

by the long-time algebraic decay (see above), so that some phase-information persists in the system at long times.

V. DISCUSSION

In the model system examined here, phase controllability was successfully demonstrated, primarily mediated by the breaking of time-reversal symmetry, which is a completely incoherent process. Although we could not observe any significant effect of the off-diagonal elements (stationary coherences) during the control phase, the fact that it can reach large values (see Fig. 7) implies that these terms must be included in any treatment of phase control and may well be influential in other model systems.

We note that there is a fundamental difference in the nature of control mechanisms arising via the time-reversal symmetry and the stationary coherences. Specifically, the first is an effect that can arise in either classical or quantum mechanics. Indeed, proving that the origin of such experimentally observed control is quantum, e.g., via a Bell inequality⁴², is far from a trivial task. By contrast, the off-diagonal elements vanish in classical mechanics³⁷. Hence, they are quantum in nature, arising from the entanglement between the system and the bath. Although in our case the contribution of the off-diagonal elements is of second order in the effective coupling to the bath¹⁹, and therefore is expected to be small, any successful observation of the role of the off-diagonal elements in OPPC will signal a pure quantum effect.

Indeed, it should be noted that, to date, there is no experimental demonstration of environmentally assisted one photon phase control. The original⁷⁻⁹ or related experiments⁴³ in which this mechanism was invoked, as well as the related computational work¹⁶, showed phase control of *cis-trans* isomerization. However, the property “cis-or-trans” consists of a projection onto a spatial domain, and hence is an operator that does not commute with the system Hamiltonian. As such, one knows^{12,17} that phase control is possible even in the absence of an environment. Rather, the environment in case of isomerization serves to relax the system into one of the two isomers. The insights afforded by the analysis in this paper should serve to motivate new studies to experimentally demonstrate one photon phase control.

ACKNOWLEDGMENTS

This work was supported by NSERC and by the US Air Force Office of Scientific Research under contract number FA9550-10-1-0260, and by *Comité para el Desarrollo de la Investigación* –CODI– of Universidad de Antioquia, Colombia under contract number E01651 and under the *Estrategia de Sostenibilidad 2013-2014* and by the *Colombian Institute for the Science and Technology Development* –COLCIENCIAS– under grant number 111556934912.

REFERENCES

- ¹M. Shapiro and P. Brumer, *Quantum Control of Molecular Processes*, 2nd ed. (Wiley-VCH, Weinheim, 2012).
- ²C.-C. Shu and N. E. Henriksen, *J. Chem. Phys.* **134**, 164308 (2011).
- ³C.-C. Shu and N. E. Henriksen, *J. Chem. Phys.* **136**, 044303 (2012).
- ⁴T. Grinev, M. Shapiro, and P. Brumer, *J. Chem. Phys.* **138**, 044306 (2013).
- ⁵M. Schlosshauer, *Decoherence and the Quantum-To-Classical Transition* (Springer-Verlag, Berlin, 2007).
- ⁶Y. Elran and P. Brumer, *J. Chem. Phys.* **138**, 234308 (2013).
- ⁷V. Prokhorenko, A. Nagy, S. A. Waschuk, L. S. Brown, R. R. Birge, and R. J. D. Miller, *Science* **313**, 1257 (2006).
- ⁸M. Joffre, *Science* **317**, 453b (2007).
- ⁹V. Prokhorenko, A. Nagy, S. A. Waschuk, L. S. Brown, R. R. Birge, and R. J. D. Miller, *Science* **317**, 453c (2007).
- ¹⁰C. Florean, D. Cardoza, J. L. White, J. K. Lanyi, R. J. Sension, and P. H. Bucksbaum, *Proc. Natl. Acad. Sci. U.S.A.* **106**, 10896 (2009).
- ¹¹G. Katz, M. A. Ratner, and R. Kosloff, *New Journal of Physics* **12**, 015003 (2010).
- ¹²M. Spanner, C. A. Arango, and P. Brumer, *J. Chem. Phys.* **133**, 151101 (2010).
- ¹³R. Kosloff, M. Ratner, G. Katz, and M. Khasin, *Procedia Chemistry* **3**, 322 (2011), 22nd Solvay Conference on Chemistry.
- ¹⁴V. I. Prokhorenko, A. Halpin, P. J. M. Johnson, R. Miller, and L. S. Brown, *J. Chem. Phys.* **134**, 085105 (2011).
- ¹⁵General Discussion, *Disc. Far. Soc.* **153**, 428 (2011).

- ¹⁶C. A. Arango and P. Brumer, *J. Chem. Phys.* **138**, 071104 (2013).
- ¹⁷L. A. Pachón, L. Yu, and P. Brumer, *Faraday Discussions* **163**, 485 (2013), arXiv:1212.6416.
- ¹⁸P. Brumer and M. Shapiro, *Chem. Phys.* **139**, 221 (1989).
- ¹⁹L. A. Pachón, J. F. Triana, and P. Brumer, Canonical Typicality Deviations at Low Temperature , In preparation. (2013).
- ²⁰L. A. Pachón and P. Brumer, *Phys. Rev. A* **87**, 022106 (2013), arXiv:1210.6374.
- ²¹X.-P. Jiang and P. Brumer, *J. Chem. Phys.* **94**, 5833 (1991).
- ²²H. Hoki and P. Brumer, *Procedia Chem.* **3**, 122 (2011).
- ²³P. Brumer and M. Shapiro, *Proc. Natl. Acad. Sci. U.S.A.* **109**, 19575 (2012).
- ²⁴L. A. Pachón and P. Brumer, *J. Math. Phys.* (submitted) (2013), arXiv:arXiv:1207.3104.
- ²⁵F. Galve, L. A. Pachón, and D. Zueco, *Phys. Rev. Lett.* **105**, 180501 (2010).
- ²⁶R. P. Feynman and A. R. Hibbs, *Quantum physics and path integrals* (McGraw–Hill, New York, 1965).
- ²⁷G.-L. Ingold, in *Coherent Evolution in Noisy Environments*, Lecture Notes in Physics, Vol. 611, edited by A. Buchleitner and K. Hornberger (Springer Berlin Heidelberg, 2002) pp. 1–53.
- ²⁸L. A. Pachón, G.-L. Ingold, and T. Dittrich, *Chem. Phys.* **375**, 209 (2010).
- ²⁹M. Shapiro and P. Brumer, *Rep. Prog. Phys.* **66**, 859 (2003).
- ³⁰R. P. Feynman and F. L. Vernon, *Annals of Physics* **24**, 118 (1963).
- ³¹A. O. Caldeira and A. L. Leggett, *Physica A* **121**, 587 (1983).
- ³²H. Grabert, P. Schramm, and G.-L. Ingold, *Phys. Rep.* **168**, 115 (1988).
- ³³U. Weiss, *Quantum Dissipative Systems*, 4th ed. (World Scientific, Singapore, 2012).
- ³⁴H. Grabert, U. Weiss, and P. Talkner, *Z. Phys. B* **55**, 87 (1984).
- ³⁵F. Haake and R. Reibold, *Phys. Rev. A* **32**, 2462 (1985).
- ³⁶P. Hänggi and G.-L. Ingold, *Chaos* **15**, 026105 (2005).
- ³⁷M. Campisi, P. Talkner, and P. Hänggi, *Phys. Rev. Lett.* **102**, 210401 (2009).
- ³⁸A Mathematica 8.0 script with the numerical implementation of the results for the Ohmic spectral density can be found at <http://gfam.udea.edu.co/~lpachon/scripts/oqsystems>.
- ³⁹P. Hänggi and P. Jung, in *Advances in Chemical Physics*, Lecture Notes in Physics, Vol. 611, edited by I. Prigogine and S. A. Rice (John Wiley & Sons, Inc., 2007) pp. 239–326.
- ⁴⁰L. A. Pachón and P. Brumer, Experimentally Accessible Determination of Spectral Densities of Molecular Complexes , In preparation (2013).

⁴¹D. Kast and J. Ankerhold, *Phys. Rev. Lett.* **110**, 010402 (2013).

⁴²T. Scholak and P. Brumer, *Phys. Rev. Lett.* , submitted (2013), [arXiv:1305.4586](https://arxiv.org/abs/1305.4586).

⁴³V. I. Prokhorenko, A. Halpin, and R. J. D. Miller, *Faraday Discuss.* **153**, 27 (2011).

Appendix A: Evolution of the density operator

The matrix \mathbf{A} contains the information about the open system evolution and is defined as

$$\mathbf{A} = \frac{1}{q_0^6 \det \mathbf{M}} \begin{pmatrix} 1 + \mathbf{A}_{11} & \mathbf{A}_{12} \\ \mathbf{A}_{12} & 1 + \mathbf{A}_{22} \end{pmatrix}, \quad (\text{A1})$$

being

$$\mathbf{A}_{11} = \frac{m^2}{\hbar^2 \omega_0^2 \Lambda^2} (1 - 2\Lambda\omega_0) \left[\frac{\dot{G}_+(t)}{G_+(t)} S(t) - \dot{S}(t) \right]^2 + (1 + 2\Lambda\omega_0) \frac{\dot{G}_+^2(t)}{\omega_0^2 G_+^2(t)} + \frac{2\Omega}{\omega_0}, \quad (\text{A2})$$

$$\mathbf{A}_{12} = \frac{m^3}{\hbar^3 \omega_0 \Lambda^2} \frac{S(t)}{G_+(t)} \left[\frac{\dot{G}_+(t)}{G_+(t)} S(t) - \dot{S}(t) \right] \left[\frac{S(t)}{G_+(t)} - 2\Lambda\omega_0 \right], \quad (\text{A3})$$

$$\mathbf{A}_{22} = \frac{m^2}{\hbar^2 \omega_0^2 \Lambda^2} (1 - 2\Lambda\omega_0) \frac{S^2(t)}{G_+^2(t)} + (1 + 2\Lambda\omega_0) \frac{1}{\omega_0^2 G_+^2(t)} - \frac{2\Omega}{\omega_0}. \quad (\text{A4})$$

Λ is related to the second moment in equilibrium of the \hat{q} by means of $\langle \hat{q}^2 \rangle = \hbar\Lambda/m$ while Ω through $\langle \hat{p}^2 \rangle = \hbar m \Omega$ ³². $S(t)$ denotes the symmetric position autocorrelation function, $S(t) = \frac{1}{2} \langle \hat{q}(t)\hat{q} + \hat{q}\hat{q}(t) \rangle$. In the limit $\omega_D \rightarrow \infty$, it is given by

$$S(t) = \frac{\hbar}{4m\omega_d} [\exp(-\lambda_2 t) \coth(\frac{1}{2}\hbar\beta\lambda_2) - \exp(-\lambda_1 t) \coth(\frac{1}{2}\hbar\beta\lambda_1)] - \Gamma(t), \quad (\text{A5})$$

$$\Gamma(t) = \frac{\gamma}{m\beta} \sum_{n=-\infty}^{\infty} \frac{|\nu_n| \exp(-|\nu_n|t)}{(\omega_0^2 + \nu_n^2)^2 - \gamma^2 \nu_n^2}, \quad (\text{A6})$$

being $\nu_n = 2\pi n/\hbar\beta$ the Matsubara frequencies (cf. Ref. 32,34).

The matrix M is given by

$$M(t) = \frac{m}{\hbar} \begin{pmatrix} R^{--}(t) & -i\frac{\dot{G}_+(t)}{G_+(t)} & -C_2^-(t) + R^{+-}(t) & i\frac{1}{G_-(t)} - iC_1^-(t) \\ -i\frac{\dot{G}_+(t)}{G_+(t)} & 0 & i\frac{1}{G_+(t)} & 0 \\ -C_2^-(t) + R^{+-}(t) & i\frac{1}{G_+(t)} & -2C_2^+(t) + R^{++}(t) & -i\frac{\dot{G}_+(t)}{G_+(t)} - iC_1^+(t) \\ i\frac{1}{G_-(t)} - iC_1^-(t) & 0 & -i\frac{\dot{G}_+(t)}{G_+(t)} - iC_1^+(t) & 0 \end{pmatrix}, \quad (\text{A7})$$

being

$$C_j^+(t) = \int_0^t ds C_j(s) \frac{G_+(t-s)}{G_+(t)}, \quad C_j^-(t) = \int_0^t ds C_j(s) \frac{G_-(s)}{G_-(t)}, \quad (\text{A8})$$

$$R^{+-}(t) = \int_0^t ds \int_0^t du R(s, u) \frac{G_+(t-s)}{G_+(t)} \frac{G_-(u)}{G_-(t)}, \quad (\text{A9})$$

with $R^{++}(t)$ and $R^{--}(t)$ defined accordingly.